Imaging and magnetometry of switching in nanometerscale iron particles

S. Gider, J. Shi, D. D. Awschalom, P. F. Hopkins, K. L. Campman, A. C. Gossard, A. D. Kent, and S. von Molnár

Citation: Applied Physics Letters **69**, 3269 (1996); doi: 10.1063/1.118032
View online: http://dx.doi.org/10.1063/1.118032
View Table of Contents: http://scitation.aip.org/content/aip/journal/apl/69/21?ver=pdfcov
Published by the AIP Publishing

Imaging and magnetometry of switching in nanometer-scale iron particles

S. Gider,[a] J. Shi, and D. D. Awschalom[b]
Department of Physics, University of California, Santa Barbara, California 93106

P. F. Hopkins, K. L. Campman, and A. C. Gossard
Department of Materials, University of California, Santa Barbara, California 93106

A. D. Kent
Department of Physics, New York University, New York, New York 10003

S. von Molnár
Center for Materials Research and Technology, Florida State University, Tallahassee, Florida 32306

(Received 29 August 1996; accepted for publication 18 September 1996)

The reversal mechanisms in arrays of nanometer-scale (<40 nm diameter) iron particles are studied by low-temperature Hall magnetometry and room-temperature magnetic force microscopy. Rotation of the net array magnetization at low temperatures (20 K) occurs by both reversible and irreversible modes, the latter revealed by Barkhausen jumps. Spatially resolved measurements at room temperature show the particles to be single domain with remanence and coercivity indicating they are not superparamagnetic. Individual particles are observed to switch irreversibly over a small field range (<10 Oe) between preferred magnetic directions parallel to the growth direction of the particles. Scaling of the arrays offers the possibility of magnetic storage at the 45 Gbit/in.^{2} level, nearly 50 times greater than current technology. © *1996 American Institute of Physics.* [S0003-6951(96)Q4547-0]

The control of anisotropy in magnetic systems is essential for technological applications requiring hysteresis curves with particular qualities. Shape anisotropy generally dominates the hysteresis of single domain particles, but the remanence and coercivity are reduced with a distribution of particle shapes and orientations.[1] Furthermore, hysteresis loops may collapse as the magnetic volume decreases and the anisotropy energy barrier becomes comparable to the available thermal energy (superparamagnetism). Work on defining the hysteresis of nanometer-scale particles has included surface chemistry modification[2] to exploit the large surface-to-volume ratio and lithographic patterning of thin films to determine the shape anisotropy.[3–7] Shape may also be controlled during growth by electrochemical deposition[7–9] and by scanning tunneling microscopy (STM) deposition. The latter techniques allow exploration down to the 10 nm scale, which is currently inaccessible by lithography. The present work employs local organometallic deposition with a STM to produce nanometer-scale iron particles with control of the shape and orientation. Previously, the magnetic properties of the STM particles were studied in ensembles at low temperature.[10] By complementary low-temperature Hall magnetometer and room-temperature magnetic force microscope (MFM) measurements, the average magnetic properties of an array of particles are now compared with the properties of individual particles. The limitations of each measurement technique are also considered.

To produce the arrays of iron particles, iron pentacarbonyl [$Fe(CO)_5$] is introduced into the ultra high-vacuum ($\sim 2\times10^{-10}$ Torr) chamber of the STM. When the tip is negatively biased with respect to the substrate, electrons field emit from the tip to the substrate, dissociate the carbonyl ligands from the organometallic, and deposit iron locally.[11,12] High aspect ratio particles are produced by maintaining a constant emission current as the tip is withdrawn. The samples are characterized *in situ* by imaging with a lower current in tunneling mode or *ex situ* by transmission electron (TEM), scanning electron (SEM), scanning Auger, and atomic force (AFM) microscopies.[12] Particles with aspect ratios in the SEM ranging from one to three are studied in the present work. Only upper limits of 40 nm in diameter and 40–120 nm in height can be established with confidence because of a carbon coating that develops during growth and/or during observation by electron probes in the presence of hydrocarbons. The existence of the carbon coating is confined by TEM and Auger analysis[12] and is consistent with subsequent magnetic measurements.[10]

The magnetic properties of the arrays of iron particles are studied at low temperatures (<100 K) with a Hall magnetometer[10] fabricated from a Be modulation doped $GaAs/Al_{0.3}Ga_{0.7}As$ heterostructure grown by molecular-beam epitaxy. At 4.5 K the structure has a carrier concentration of 3.1×10^{15} m^{-2}, yielding a sensitivity of 0.2 Ω/G and a mobility of 17 m^2/V s. An array is grown 100 nm above the $(2.5\ \mu m)^2$ square active area of a Hall cross. The sensitivity of the Hall magnetometer depends on the placement of the magnets with respect to the active area of the Hall cross. To a first approximation, the Hall voltage corresponds to the average over the active area of the perpendicular field, i.e., the average magnetic flux. Magnets at the corners of the active area (the lowest points of symmetry) couple the least amount of return flux and therefore give a larger contribution to the Hall voltage (Fig. 1). For an array of magnets, the maximum flux coupling is achieved for complete coverage of the sensing area. Tilting of the magnetic moments can lead to negative flux coupling from dipoles at an edge of the active area and hysteresis loops which are difficult to interpret. Therefore, all measurements are performed with the external field applied perpendicular to the active area of the Hall magnetometer (henceforth known as the vertical direc-

[a]Present address: IBM Almaden Research Center, D1, 650 Harry Road, San Jose, CA 95120.
[b]Electronic mail: awsch@lotemp.physics.ucsb.edu

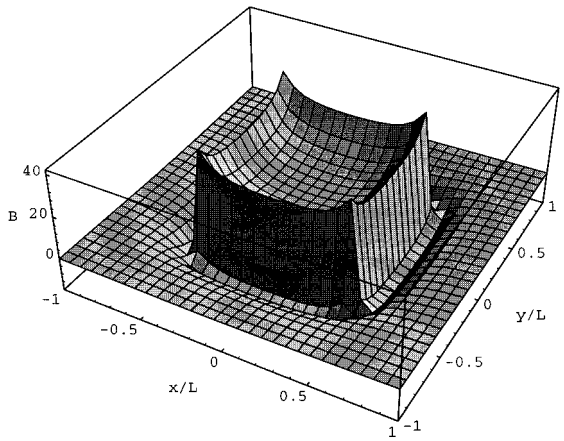

FIG. 1. The height B of the surface at (x,y) represents the average z component of the field over an $L\times L$ area due to a dipole at (x,y,z), where $z/L=0.04$ in this case. The dipole is oriented perpendicular to the area ($\vartheta=0°$).

tion). The observed noise level is equivalent to the signal produced by a dipole of $\sim 10^{-13}$ emu located at the center of the active area and oriented with its moment perpendicular to the plane of the active area.

Insight about the magnetization reversal process can be gained by a measurement of the switching field, the field at which the rotation of the moments becomes irreversible. Following positive saturation the field is reversed, but before the hysteresis loop attains negative saturation the field is reversed again. The field at which the hysteresis loop does not retrace itself is the switching field, at which there is a kink in the hysteresis loop [Fig. 2(a)]. Switching of the particles is probed further by traversing the irreversible part of the loop slowly [Fig. 2(b)]. Magnetization reversal there tends to occur by Barkhausen jumps rather than by continuous rotation moments. Repeated sweeps show more variation in the irreversible part of the loop than in the reversible part. The irreproducibility of the discrete jumps could either be due to domain-wall motion over a variable energy landscape[13] or random switching of single domain particles. Magnetic force imaging supports the latter interpretation. Because of the variation in the coupling strength of the dipoles to the Hall voltage due to geometrical effects (Fig. 1), it is difficult to determine the exact number of particles switching at each jump. An estimate is nevertheless possible by dividing the height of the loop (140 G) by the total number of particles in the array ($\sim$500). The 0.3 G signal from the reversal of one particle is slightly above the noise level of 0.2 G. Therefore, the identification of parts of the loop as reversible and irreversible can be made without question. Since the reversible parts occurs over a large fraction of the measured loop, irreversible changes cannot be concealed in the noise.

While a Hall magnetometer measures the average properties of the arrays, a MFM resolves the magnetic state of individual particles and simultaneously provides topographic information. The sensing element of the commercial MFM[14] is a single-crystal silicon cantilever whose tip is coated with a magnetic film. This film consists of 50 nm of CoCr with an effective moment of $\sim 10^{-12}$ emu and a coercive field of $\sim$500 Oe. The external field is applied vertically in order to make a direct comparison with the Hall measurements. In

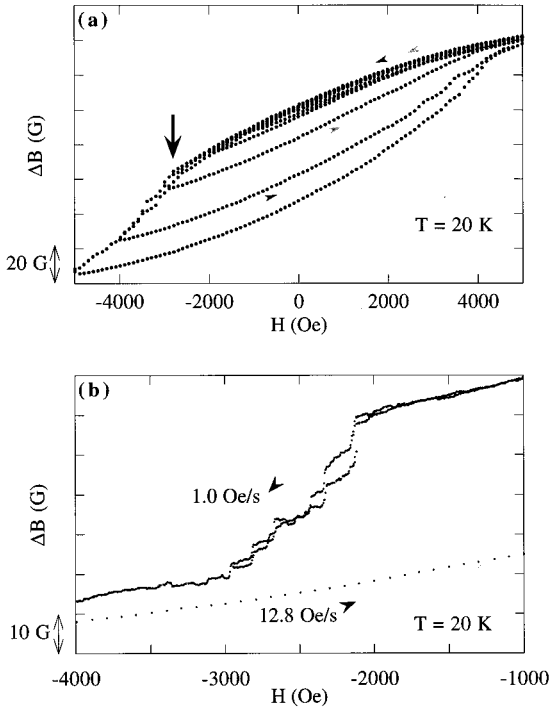

FIG. 2. (a) The large arrow indicates the switching field as measured with the Hall magnetometer by successively negative field sweeps in steps of 1000 Oe. (b) A detail of the negative half of the hysteresis loop for two field sweeps. The rate of decreasing field is slower to show the discrete jumps.

addition, a vertically magnetized tip gives the most unambiguous images.[15] The actual field experienced by the particles will be a sum of the external field and the tip field. At the detection height ($\sim$20 nm) above the surface for magnetic force imaging, the tip field can be as large as several hundred Oe, but the sample will also experience a larger intermittent field from the tip during the topography imaging as the tip scans over the sample in tapping mode. This can been seen in particles switched by the tip, the half-light and half-dark particles with the division parallel to the horizontal scan direction [Fig. 3(b)]. Another interesting result from the MFM measurements is that the iron particles show remanent magnetization at room temperature, demonstrating that they are not superparamagnetic at these temperatures. Furthermore, the magnetic moments of the particles appear to have a preferred orientation either parallel or antiparallel to the growth direction. Note that a dark circle surrounded by a light ring in the magnetic force image corresponds to a particle magnetized parallel to the tip.[15] More important, a particle oriented normal to the tip will show multiple lobes.

To study the reversal mechanism of the iron particles, the MFM is repeatedly scanned over a particular row while ramping the external field (Fig. 4). The sample is initially saturated with a field of 1 kOe opposite the tip magnetization. In this process the tip is withdrawn in order that the sample and tip remain in opposite directions. However, after this procedure the remanent states of the particles are not uniformly opposite the tip (bottom of Fig. 4), because the tip field alone is sufficient to reverse some of the particles. Thus, it is difficult to measure the absolute coercive fields of the particles; nevertheless, the characteristic sudden switching of single domain particles is observed as the external field is

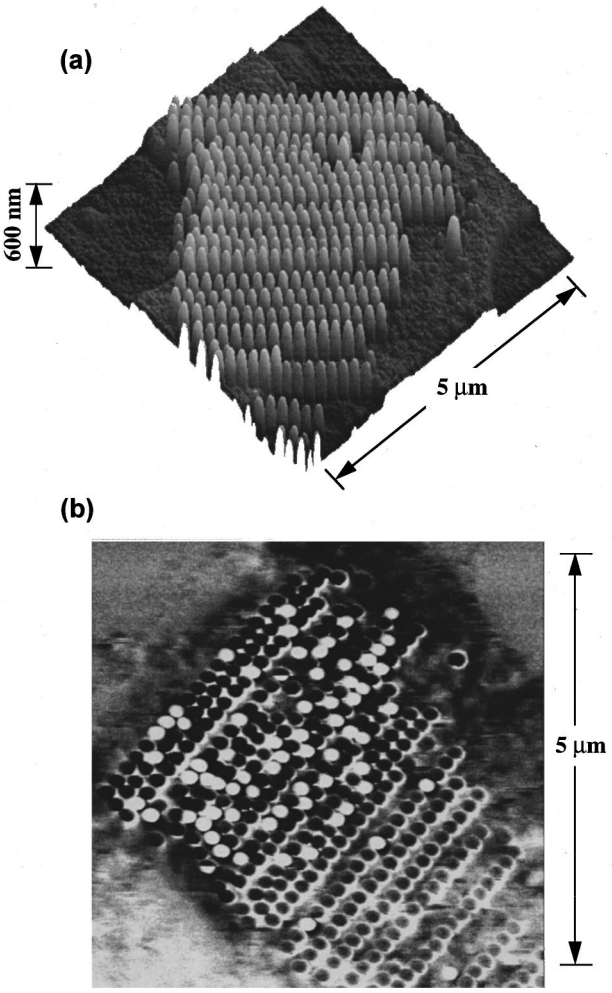

FIG. 3. (a) Atomic force image of an array of particles within a Hall cross. (b) Magnetic force image of the same array taken at a 30 nm lift height. The gray-scale range represents a 3° shift of phase between the drive and response of the MFM cantilever.

increased. This is consistent with the discreteness of the slow field sweeps observed with the Hall magnetometer. Unlike the hysteresis loops obtained with the Hall magnetometer, however, the magnetic force images do not show a reversible rotation of the moments, which would be revealed in gradual change in the contrast of particles in Fig. 4 from light to dark.[15] The higher temperature of the magnetic force measurements as compared to the Hall bar measurement (300 K vs 20 K) provides more thermal energy for the moments to overcome anisotropy energy barriers and thus may not allow for a stable arrangement of the moments at an angle from the easy axis. Within the spatial resolution of the MFM it is not possible to discern whether the magnetization reversal is occurring by a coherent (uniform reversal of the magnetic moments) or an incoherent mode (e.g., nucleation and rapid motion of a domain wall). While the particles appear structurally similar in the topographic images, the magnetic force image (Fig. 4) shows that the coercive fields of the particles are not the same. The true shapes of the particles may be more variable than revealed through the carbon coating and/or shape may not be the only source of magnetic anisotropy.

In conclusion, the possibility of individually addressable 40 nm bits has been demonstrated. At the spacing of 120 nm,

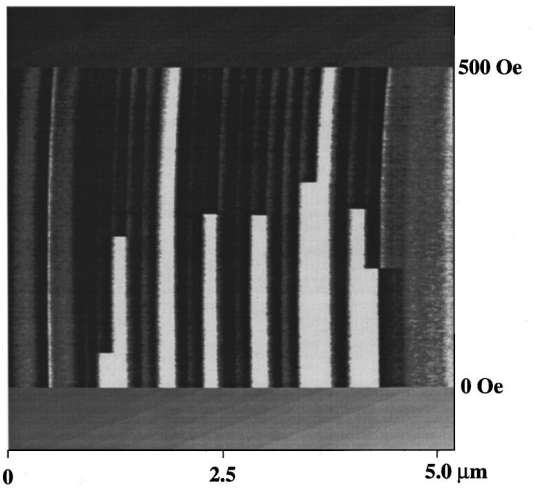

FIG. 4. While ramping the field, the scan is repeated for the 21 particles in the third row from the top in the previous figure. The whole image is acquired in 250 s with 10 Oe field steps. Thermal drift induced by heat from the electromagnet skews the image at high fields.

the density would be 45 Gbits/in^2. The practical realization of a storage technology at this level would obviously require higher rates of deposition for scaling the arrays over larger areas and higher data rates for reading than are currently available with scanning probes. Parallel arrays of scanning probes may overcome current scanning probe bandwidth limits. Improvement is also necessary in the control of the magnitude of the anisotropy of particles. Although the STM forms particles that are ostensibly similar in structure with a preferred anistropy direction, there is found to be a distribution of coercive fields. Magnetic properties may thus serve as a more sensitive characterization of nanometer-scale particles. The Hall magnetometer provides a measure of the average magnetic properties of nanometer-scale particles, but requires care in interpretation since particles are not weighted equally. Imaging of individual particles with a MFM shows the effect of the scanning tip on small particles can be significant. Another outstanding challenge is the development of local magnetic probes which are less invasive.

This work is supported by the AFOSRF49620-96-1-0118, NSFDMR 95-27553 and -10518, and the NSF Center for Quantized Electronic Structures DMR-91-20007.

[1] E. C. Stoner and E. P. Wohlfarth, Philos. Trans. R. Soc. London, Ser. A **240**, 599 (1948).
[2] F. E. Spada, A. E. Berkowitz, and N. T. Prokey, J. Appl. Phys. **69**, 4475 (1991).
[3] J. F. Smyth *et al.*, J. Appl. Phys. **69**, 5262 (1991).
[4] R. M. H. New, R. F. W. Pease, and R. L. White, J. Vac. Sci. Technol. B **13**, 1089 (1995).
[5] W. Wernsdorder *et al.*, J. Magn. Magn. Mater. **145**, 33 (1995).
[6] P. D. Ye, D. Weiss, K. von Klitzing, and K. Eberl, Appl. Phys. Lett. **67**, 1441 (1995).
[7] S. Y. Chou, P. R. Krauss, and L. Kong, J. Appl. Phys. **79**, 6101 (1996).
[8] J. Meier, B. Doudin, and J.-Ph. Ansermet, J. Appl. Phys. **79**, 6010 (1996).
[9] R. O'Barr, *et al.*, J. Appl. Phys. **79**, 5303 (1996).
[10] A. D. Kent, S. von Molnár, S. Gider, and D. D. Awschalom, J. Appl. Phys. **76**, 6656 (1994).
[11] M. A. McCord and D. D. Awschalom, Appl. Phys. Lett. **57**, 2153 (1990).
[12] A. D. Kent, T. M. Shaw, S. von Molnár, and D. D. Awschalom, Science **262**, 1249 (1993).
[13] H. Weinstock, T. Erber, and M. Nisenoff, Phys. Rev. B **31**, 1535 (1985).
[14] Digital Instruments, Santa Barbara, CA 93103.
[15] J. Shi, S. Gider, K. Babcock, and D. D. Awschalom, Science **271**, 937 (1996).